TÜBİTAK

Turkish Journal of Physics

http://journals.tubitak.gov.tr/physics/

Research Article

Turk J Phys
(2017) 41: 143 – 150
© TÜBİTAK
doi:10.3906/fiz-1610-28

Promising features of $In_{0.5}Ga_{0.5}N/Al_{0.2}Ga_{0.8}N$ quantum dot lasers

Halima BOUCHENAFA[1,2,*], **Badra BOUABDALLAH**[3], **Boucif BENICHOU**[2]
[1]Department of Physics, Faculty of Exact Sciences and Informatics, University Hassiba Ben Bouali of Chlef, Chlef, Algeria
[2]Department of Physics, Faculty of Exact Sciences, University Djillali Liabès of Sidi Bel Abbès, Sidi Bel Abbès, Algeria
[3]Condensed Matter and Sustainable Development Laboratory, University Djillali Liabès of Sidi Bel Abbès, Sidi Bel Abbès, Algeria

Received: 25.10.2016 • **Accepted/Published Online:** 09.12.2016 • **Final Version:** 18.04.2017

Abstract: The group-III nitrides, InN, GaN, and AlN, and their alloys have emerged as one of the most important material classes for optoelectronic devices. The incorporation of quantum dots (QDs) as active material improves the performance of conventional optoelectronic devices, such as laser diodes. In this study, we present a theoretical analysis of the gain characteristics of $In_xGa_{1-x}N/Al_{0.2}Ga_{0.8}N$ three-dimensional quantum box lasers, based on the density matrix theory of semiconductor lasers with relaxation broadening. The study is done on three samples of QDs: $GaN/Al_{0.2}Ga_{0.8}N$, $In_{0.3}Ga_{0.7}N/Al_{0.2}Ga_{0.8}N$, and $In_{0.5}Ga_{0.5}N/Al_{0.2}Ga_{0.8}N$. A comparative study of the gain spectra of $GaN/Al_{0.2}Ga_{0.8}N$-based quantum-well and QD lasers is also presented for various side lengths. The variation of peak gain on carrier density is presented as well. The effect of indium composition on the variation in modal gain versus current density and the threshold current with inverse cavity length is plotted. The results show that the $In_{0.5}Ga_{0.5}N/Al_{0.2}Ga_{0.8}N$ QD laser emitting at red wavelength has a higher value of optical gain of 19,575 cm^{-1} and a lower threshold current density of 143.9 A/cm^2.

Key words: Quantum dot, quantum-well lasers, optical gain, nitride semiconductors

1. Introduction

Quantum dots (QDs) are 3-dimensionally confined quantum structures [1]. They are entities of great interest for the development of new devices. Lasers with QDs embedded in the active layer are predicted to improve the characteristics of lasers, such as suppression of temperature dependence of the threshold current, a reduced threshold current density, and a reduced total threshold current [2].

The use of QDs in nitride semiconductors is more effective, since the zero-dimensional electronic states in the QDs play an essential role for improving optical gain and threshold current characteristics, particularly in wide band-gap semiconductors [3].

Nitride-based semiconductors GaN, AlN, and InN have been successfully applied in laser diodes thanks to their intrinsic material properties such as a direct transition band structure. The band gap energy ranges from 0.7 eV for InN and 3.4 eV for GaN to 6.2 eV for AlN [4]. By adding indium and aluminum to GaN, ternary alloys can be formed with wide bandgap ranges of from 0.7 to 6.2 eV, which can cover the spectral range from deep ultraviolet (UV) to infrared (IR) at room temperature [5,6].

*Correspondence: bouchenafa_halima@yahoo.fr

In this paper, we analyze the optical gain and threshold performances of the $In_xGa_{1-x}N/Al_{0.2}Ga_{0.8}N$ three-dimensional QD lasers based on the density matrix theory of semiconductor lasers with relaxation broadening [7].

The optical gain and threshold current density represent the basic elements that must be optimized to produce a high performance quantum box laser and are also important elements in the comparison of three materials-based nitride quantum dots ($GaN/Al_{0.2}Ga_{0.8}N$, $In_{0.3}Ga_{0.7}N/Al_{0.2}Ga_{0.8}N$, and $In_{0.5}Ga_{0.5}N/Al_{0.2}Ga_{0.8}N$).

2. Theoretical background

The behavior of semiconductor-based lasing heterostructures is characterized by optical gain and threshold current, which are very basic and important parameters.

2.1. Optical gain

The optical gain of the QD active region based on the density-matrix theory is calculated from the following relation [7]:

$$g(\omega) = \frac{\omega}{n_r}\sqrt{\frac{\mu_0}{\varepsilon_0}}\sum_{lmn}\int_{E_g}^{\infty}\langle R_{cv}^2\rangle \frac{g_{cv}\left(f_c - f_v\right)\hbar/\tau_{in}}{\left(E_{cv} - \hbar\omega\right)^2 + \left(\hbar/\tau_{in}\right)^2} dE_{ch}, \tag{1}$$

where f_c and f_v are the corresponding Fermi functions for electrons in the conduction and valence bands. E_{cv} is a transition energy between the conduction band and valence band, R_{cv} is the dipole moment, ω is the angular frequency of light, ε_0 and μ_0 are respectively the dielectric constant and permeability of the vacuum, τ_{in} is the intraband relaxation time ($\tau_{in} = 0.1\,ps$), n_r is the refractive index, and g_{cv} is the density of states for the QD, given by [7]:

$$g_{cv}\left(E_{cv}\right) = \frac{2\delta\left(E_{cv} - E_{cnml} - E_{vnml} - E_g\right)}{L_x L_y L_z}, \tag{2}$$

where L_x, L_y, and L_z are the well widths along the x, y and z directions, respectively; δE is the delta function; and E_{cnml} and E_{vnml} are the quantized energy levels [8].

In Eq. (1), we have supposed that the electron and the hole in the quantum box are in equilibrium determined by quasi-Fermi levels E_{fc} and E_{fv}, respectively.

E_{fc} and E_{fv} are related to the electron and hole densities injected into the quantum box as follows [7,9]:

$$N = \sum_{nml}\frac{2}{\left[1 + \exp\left(\frac{E_{cnml} - E_{fc}}{kT}\right)\right] L_x L_y L_z}, \tag{3a}$$

$$P = \sum_{nml}\frac{2}{\left[1 + exp\left(\frac{E_{fv} - E_{vnml}}{kT}\right)\right] L_x L_y L_z}. \tag{3b}$$

In the approach of Eqs. (1), (3a), and (3b), we have assumed the transition from the first conduction band to the first valence band (heavy hole band) because the density of states of the light hole band is smaller than that of the heavy hole band and its probability to occur is more significant than the other transitions.

2.2. Threshold current density

The threshold carrier density is calculated using the following equation [10]:

$$N_{th}=N_{tr}+\frac{1}{\Gamma a}\left(\alpha_i+\frac{1}{2L_c}ln\left(\frac{1}{R}\right)\right), \tag{4}$$

where α_i is internal loss, a is differential gain, Γ is optical confinement factor, L_c is cavity length, and N_{tr} is transparency carrier density.

The threshold current density using threshold carrier density (N_{th}) is written as [7]:

$$J_{th} = \frac{n\eta q L_z N_{th}}{\tau_s}, \tag{5}$$

where q is electron charge, η is the rate of the surface area of quantum boxes included in the whole area, n is the number of the layers of the quantum box array, and τ_s is carrier life time.

3. Results and discussion

We present in this section the results of optical gain and threshold current density calculations on $In_xGa_{1-x}N$ /$Al_{0.2}Ga_{0.8}N$ QD devices, including a discussion of modal gain. It is assumed that the QD structure studied has $In_xGa_{1-x}N$ in the form of a cubic active layer of L side length ($L = L_x{=}L_y{=}L_z$) sandwiched between $Al_{0.2}Ga_{0.8}N$ barriers (Figure 1). Using a quantum box model we calculate QD quantized energy levels for conduction and valence bands, which are implemented in the model described below to calculate the optical gain. The different parameters used for calculation are gathered in Table 1.

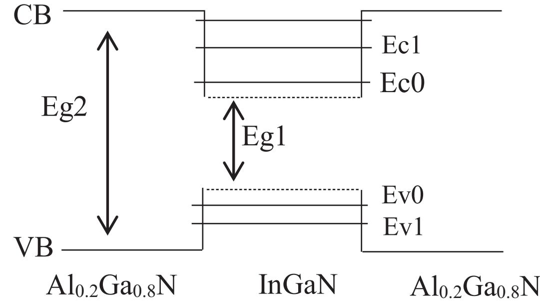

Figure 1. One-dimensional scheme of the band diagram of InGaN-based quantum dot. CB: Conduction band; VB: valence band; Eg1: band gap of InGaN; Eg2: band gap of $Al_{0.2}Ga_{0.8}N$. Ec0/Ev0 are ground quantized energy levels of electron and hole in CB and BV, respectively.

Table 1. Alloy data used in calculations (m_0 is the free electron mass).

	GaN	$In_{0.3}Ga_{0.7}N$	$In_{0.5}Ga_{0.5}N$
Band gap energy (Eg (eV))	3.43	2.305	1.715
Electron effective mass (m_e)	0.2 m_0	0.167 m_0	0.135 m_0
Heavy hole effective mass (m_{hh})	0.8 m_0	1.049 m_0	1.215 m_0
Refractive index n_r	2.67	2.784	2.86
Spin orbit splitting Δ_{cr} (eV)	0.019	0.0108	0.008

Figure 2 presents a comparison between the optical gain spectra of the GaN QD and quantum-well (QW) structures for different sizes of QW and QD at N_v= 3.10^{19} cm^{-3}, where we observe a higher optical gain value of the quantum box compared to that of the QW for the same sizes.

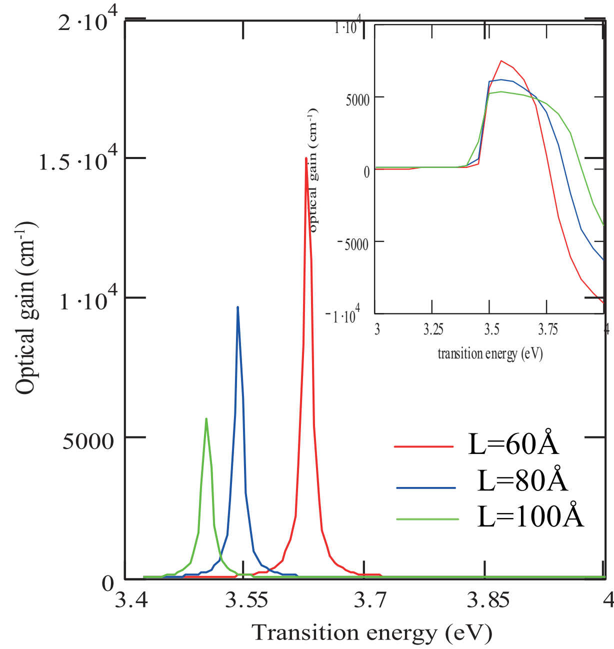

Figure 2. Optical gain versus transition energy of $In_xGa_{1-x}N$ QD structures for different sizes of quantum box at $N_v = 3.10^{19}$ cm^{-3}, x = 0. The inset shows the same gain spectra of $In_xGa_{1-x}N$ QW structures.

We also note on spectra of the quantum box that the gain increases with the decrease of the size of the QD: it is higher at $L = 60\,\mathring{A}$ compared to other lengths due to the increase of carrier density for population inversion in small-sized quantum boxes. On the other hand, when the size of the QD increases, the carriers in the box are distributed over useless levels and the separation between energy levels is not enough to obtain high gain.

We summarize the maximum gain and the peak transition energy observed in Figure 2 for an injected carrier density, $N_v = 3.10^{19}$ cm^{-3}, at T = 300 K in Table 2.

Table 2. Comparative table of values of the maximum gain and peak transition energy of GaN-based quantum box and well for different sizes.

	Gain max (cm^{-1})			Peak transition energy (eV)		
	L = 60 Å	L = 80 Å	L = 100 Å	L = Å	L = 80 Å	L = 100 Å
BQ	15,413	9684.5	5667.5	3.626	3.54	3.5
QW	7429	6195	5225.6	3.55	3.53	3.525

In Figure 3 the calculated material gain spectra for $In_xGa_{1-x}N$ QD structures are shown for various indium compositions. An increment in the transition energies (which is between 1.8 and 3.6 eV) is seen with the decrease of indium content.

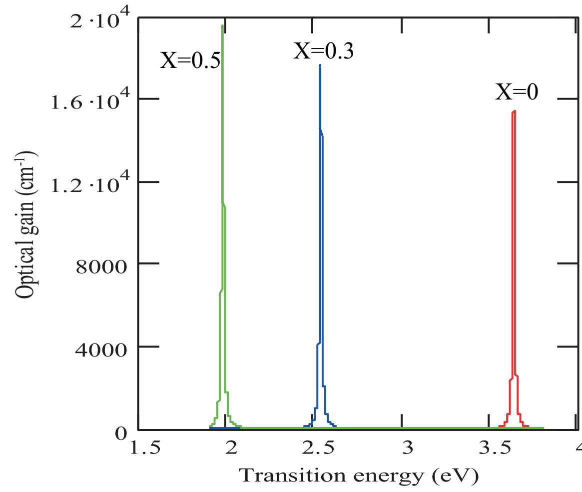

Figure 3. Optical gain versus transition energy for $In_xGa_{1-x}N$ QD structures at $N_v = 3.10^{19}\mathrm{cm}^{-3}$, $L = 60\,\mathring{A}$.

Figures 4 and 5 show the variation of maximum gain as a function of carrier density for different values of the quantum box's size and indium composition, respectively. They show two regions (positive side) and absorption (negative side) and that gives us the value of the transparency density N_{tr} from which the material begins to amplify the photon whose energy satisfies the conduction of Bernard and Duraffourg ($E_g < h\upsilon < E_{fc} - E_{fv}$) for each box size (where $h\upsilon$ is photon energy).

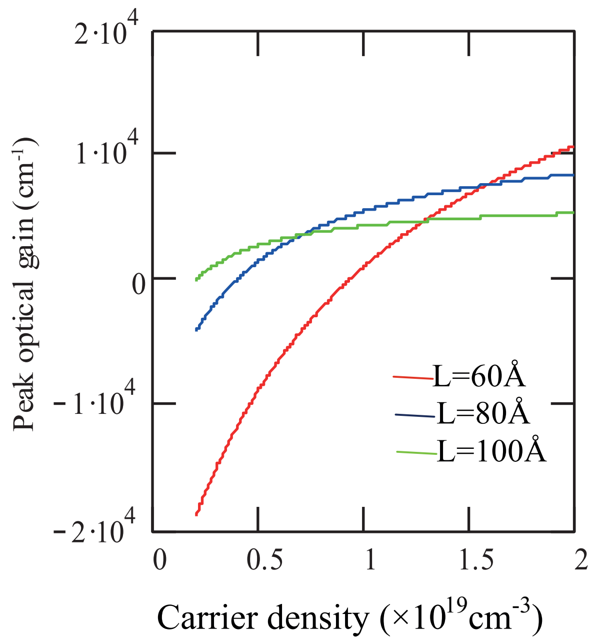

Figure 4. Dependence of peak optical gain on carrier density in $In_xGa_{1-x}N$ quantum dot at $N_v = 3.10^{19}\,\mathrm{cm}^{-3}$, x = 0.

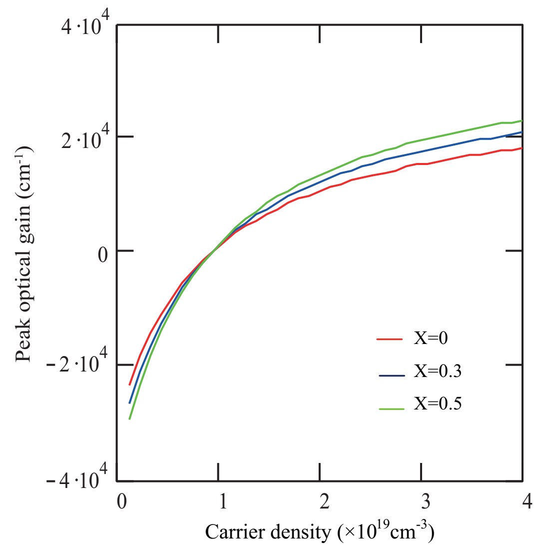

Figure 5. Dependence of peak optical gain on carrier density in $In_xGa_{1-x}N$ quantum dot at $N_v = 3.10^{19}\,\mathrm{cm}^{-3}$, $L = 60\,\mathring{A}$.

The modal gain is also a fundamental characteristic for lasing action in heterostructures. It is obtained by multiplying optical gain by the confinement factor. When the modal gain overcomes the total loss, the lasing action takes place. It is expressed as $g_m = \Gamma g$ where Γ is the optical confinement factor.

The variation of modal gain on current density values with different indium compositions for $L = 60\,\mathring{A}$ is shown in Figure 6. From this figure we observe a parabolic increase for initial values of the current density but it saturates afterwards, indicating very small or negligible increase in modal gain with change in current density. We note also that the transparency current density J_{tr} (intercept at gain = 0), which is the value at which the active layer neither absorbs nor amplifies the light at the lasing wavelength, decreases with the increase of the indium composition. Moreover, the slope of the gain versus current density plot decreases with the increasing of the indium composition.

For laser oscillation, the modal gain must equal the total losses α_{total}. The laser oscillation condition is given as [11,12,13]:

$$G_{mod} = \Gamma g_{th} = \alpha_i + \frac{1}{2L_c} ln\left(\frac{1}{R}\right) = \alpha_{total}. \tag{6}$$

The threshold current density J_{th} that corresponds to the modal gain value that satisfies the oscillation condition can be obtained from the modal gain-current density plots [14,15]. The variation of threshold current density on inverse cavity length for various values of indium composition (x) is shown in Figure 7, assuming that $\alpha_i = 5\,\text{cm}^{-1}$, $R = 0.3$, $n = 1$, and $L_c = 1.2$ mm. It is clear from the graph that the threshold current density increases with increase in reciprocal cavity length as a result of proportional increase of mirror loss. From this figure, we can deduce the differential gain a, which measures the rate with which the optical gain increases as the current is increased, and the transparency current density, J_{tr}.

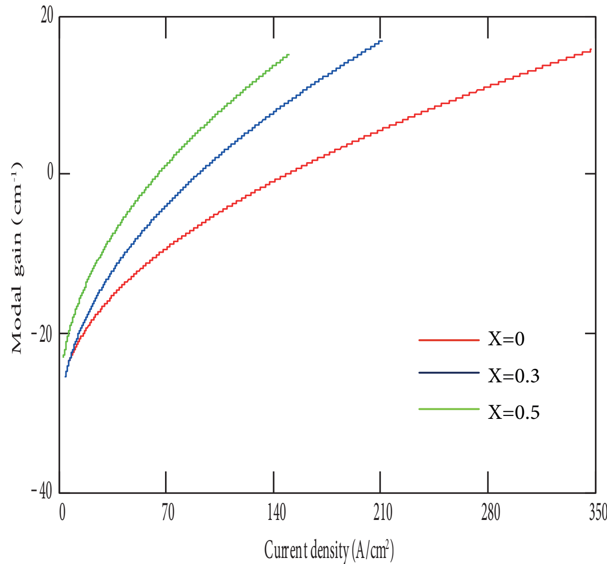

Figure 6. Modal gain as function of current density for $In_x Ga_{1-x} N/Al_{0.2} Ga_{0.8} N$ QD structures at $L = 60\,\mathring{A}$ and $N_v = 3.10^{19}\,\text{cm}^{-3}$.

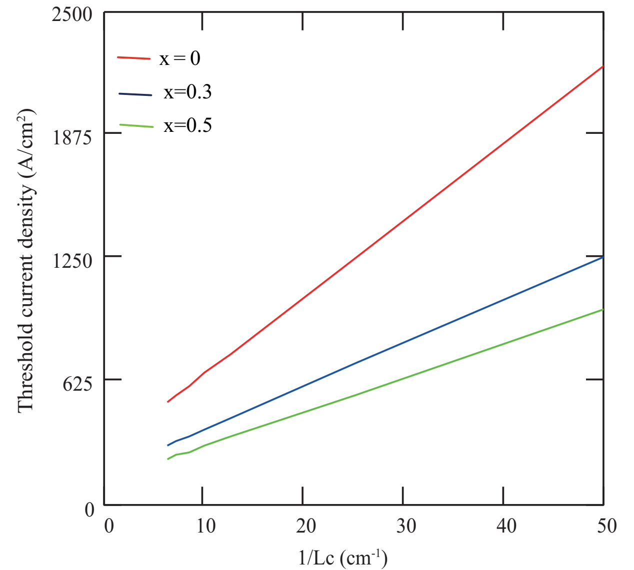

Figure 7. Threshold current density versus reciprocal cavity length for $In_x Ga_{1-x} N$ QD structures for different indium composition at $L = 60\,\mathring{A}$ and $N_v = 3.10^{19}\,\text{cm}^{-3}$.

We summarize the results obtained in this work in Table 3.

Table 3. Performance characteristics of GaN-, $In_{0.3}Ga_{0.7}N$-, and $In_{0.5}Ga_{0.5}N$-based quantum box laser (with barrier of $Al_{0.2}Ga_{0.8}N$) for $L = 60\,\AA$ and injection carrier of $3.10^{19}\,cm^{-3}$.

	$GaN/Al_{0.2}Ga_{0.8}N$	$In_{0.3}Ga_{0.7}N/Al_{0.2}Ga_{0.8}N$	$In_{0.5}Ga_{0.5}N/Al_{0.2}Ga_{0.8}N$
Gain max (cm^{-1})	15,413	17,666	19,575
Transition energy (eV)	3.626	2.53	1.973
Peak wavelength (nm)	342	490	628
Emission spectrum	UV	Blue	Red
N_{tr} ($\times 10^{19}$ cm^{-3})	0.926	0.926	0.926
Transparency current J_{tr} (A/cm^2)	148.37	90	64
Threshold current density J_{th} (A/cm^2)	323.8	187.3	143.9

From these curves and Table 3, we can deduce that the optimum structure for $In_xGa_{1-x}N$-based QD lasers is $In_{0.5}Ga_{0.5}N$ emitting at 628 nm. This choice is justified for two main reasons: the higher value of the optical gain, 19,575 cm^{-1}, and the minimum value of threshold current density of about 143.9 A/cm^2 per layer.

4. Conclusion

The calculation and analysis of laser optical gain and threshold current curves is a powerful technique for predicting the performance of any laser structure. In this work, we have investigated the optical gain characteristics of $In_xGa_{1-x}N/Al_{0.2}Ga_{0.8}N$ QD laser and the effects of the size of the QD (and size of $In_xGa_{1-x}N$ based QW for comparison) and indium composition on its performance. We have also presented the modal gain characteristics of $In_xGa_{1-x}N/Al_{0.2}Ga_{0.8}N$ QDs. The variation in modal gain with increasing current density and the threshold current density with the reciprocal cavity length have been plotted with the effect of indium composition. The present results indicate that better performance can be achieved with $In_{0.5}Ga_{0.5}N/Al_{0.2}Ga_{0.8}N$ QD lasers compared to $GaN/Al_{0.2}Ga_{0.8}N$ and $In_{0.3}Ga_{0.7}N/Al_{0.2}Ga_{0.8}N$.

References

[1] Bimberg, D.; Grundmann M.; Ledentsov, N. N. *Quantum Dot Heterostructures*; Wiley: New York, NY, USA, 1999.

[2] Nakamura, S.; Senoh, M.; Nagahama, S.; Iwasa, N.; Yamada, T.; Matsushita, T.; Kiyoku, H.; Sugimoto, Y.; Kozaki, T.; Umemoto, H. et al. *Jpn. J. Appl. Phys.* **1997**, *36*, L1568-L1571.

[3] Mukai, T.; Yamada, M.; Nakamura, S. *Jpn. J. Appl. Phys.* **1999**, *38*, 3976-3981.

[4] Zhang, L. PhD, Department of Physics and Astronomy, Katholieke Universiteit Leuven, Leuven, Belgium, 2013 (in Dutch).

[5] Al-Husseini, H.; Al-Khursan, A. H.; Al-Dabagh, S. Y. *Open Nanoscience Journal* **2009**, *3*, 1-11.

[6] Frost, T. A. PhD, Department of Electrical Engineering, University of Michigan, Ann Arbor, MI, USA, 2016.

[7] Asada, M.; Miyamoto, Y.; Suematsu, Y. *IEEE J. Quantum Electron.* **1986**, *22*, 1915-1921.

[8] Chukwuocha, E. O.; Onyeaju, M. C. *Int. J. Scientific. Technol. Res.* **2012**, *1*, 21-24.

[9] Al-Mossawi, K. H. *Opt. Photonics J.* **2011**, *1*, 65-69.

[10] Choi, H. K.; Wang, C. A.; Eglash, S. J. *Lincoln Laboratory Journal* **1990**, *3*, 395-411.

[11] Su, G. L.; Frost, T.; Bhattacharya, P.; Dallesasse, J. M.; Chuang, S. L. *Opt. Express* **2014**, *22*, 22716-22729.

[12] Sharma, M.; Yadav, R.; Lal, P.; Rahman, F.; Alvi, P. A. *Advances in Microelectronic Engineering* **2014**, *2*, 27-32.

[13] Thaira, Z. A.; Sahan, J. M. *International Journal of Advancements in Research & Technology* **2014**, *3*, 94-103.

[14] Hadjaj, F.; Belghachi, A.; Helmaoui, A. *Sensors & Transducers* **2015**, *192*, 90-95.

[15] Lu, Q.; Zhuang. Q.; Krier, A. *Photonics* **2015**, *2*, 414-425.